Progress In Electromagnetics Research, PIER 50, 209–229, 2005

A COMPLETE FDTD SIMULATION OF A REAL GPR ANTENNA SYSTEM OPERATING ABOVE LOSSY AND DISPERSIVE GROUNDS

D. Uduwawala [†], **M. Norgren, and P. Fuks**

Division of Electromagnetic Theory
Royal Institute of Technology
SE 100 44, Stockholm, Sweden

A. Gunawardena

Department of Electrical Engineering
University of Peradeniya
Peradeniya, Sri Lanka

Abstract—The finite difference time domain (FDTD) method is used to analyze a practical ground penetrating radar (GPR) antenna system operating above lossy and dispersive grounds. The antenna is of the resistor-loaded bow-tie type and the analysis is made for two known soil types, namely Puerto Rico and San Antonio clay loams. The soil is modeled by a two term Debye model with a static conductivity and it is matched to the mentioned soils by using curve fitting. The FDTD scheme is implemented by the auxiliary differential equation (ADE) method together with the uniaxial perfectly matched layer (UPML) absorbing boundary conditions (ABC). In order to model a real GPR environment, ground surface roughness and soil inhomogeneities are also included. The effect of soil properties on the GPR response and antenna input impedance is presented. Thus the ability to detect buried metal and plastic pipes is investigated.

[†] Also with Department of Electrical Engineering, University of Peradeniya, Peradeniya, Sri Lanka

1. INTRODUCTION

The realistic modeling of a ground penetrating radar (GPR) system has to deal with many aspects such as broadband antennas, lossy and dispersive media in the ground, ground surface roughness, and natural clutter like rocks and twigs. Numerical simulations of GPR systems are particularly important for the development of signal detection techniques, GPR antennas, and detection algorithms. The finite difference time domain (FDTD) [1] method is a powerful numerical technique which is widely used for this type of applications. It has the capability of modeling lossy and dispersive material as well as antennas [2, 3].

The aim of this paper is to make an FDTD simulation of a realistic, pulse driven GPR system. The antenna is of the resistor-loaded bow-tie type, a widely used broadband antenna. Lump resistors are connected at the ends of bow-tie arms to achieve broadband properties. Two such identical antennas screened with rectangular conducting cavities are used: one for transmission and the other for reception. The analysis is done when the antennas are operating above two different soil types (Puerto Rico and San Antonio clay loams) of which the conductivity and dispersive properties are known [4]. Ground surface roughness and inhomogeneities in soil are also included to simulate a real application. The radar detects the scattered signal of a buried pipe which can be either metallic or plastic.

In many published papers [5–7], GPR systems operating above lossy and dispersive soil have been simulated without considering antennas which are actually used. Therefore, the actual voltage waveform induced in the receiving antenna is unknown. The

identification of the scattered signal of the target in this waveform is highly dependent on how well the input pulse is transmitted by the antenna. Bourgeois & Smith [8] have done a complete FDTD simulation including dispersion in the ground and a commercially used GPR antenna, but without using absorbing boundary conditions (ABC). Therefore, time windowing and subtraction are needed to calculate the scattered signal of the target. This does not always give accurate results and some important properties like the input impedance of the antenna cannot be found. Also the soil is represented by a low frequency approximation of a single term Debye model.

In contrast, this paper presents a complete FDTD simulation including ABC and covers real ground conditions and broadband antennas in the GPR scenario. The soil is modeled by a two term Debye model with a static conductivity. The model parameters are found by curve fitting the model to the experimental data of the soil [4] over the frequency range of operation (i.e., DC-2 GHz). The FDTD scheme is implemented in the dispersive media by using the auxiliary differential equation (ADE) method [9, 10]. Uniaxial perfectly matched layer (UPML) [11–13] is used as the ABC to truncate the computational domain. Moreover, the 'one way injector model' [14] is used as the feed model in both the transmitting and the receiving antennas.

This paper describes how the GPR response is affected by the moisture content in the soil, the ground surface roughness and the soil inhomogeneities. The effect of dispersive ground on the antenna input impedance is also investigated. Moreover, target signatures and polarization properties of buried pipes are described.

2. GPR ANTENNA, MODELING OF SOIL, AND THE FDTD ALGORITHM

Two identical antennas of resistor-loaded bow-tie type are used for transmission and reception. Fig. 1 shows the geometry. Four lump resistors connected at the corners of the bow-tie arms, suppress the reflection of the input signal at the ends of the antenna. This gives broadband input impedance properties to the antenna so that the sharp input pulse signal can be transmitted with little distortion, an important requirement in subsurface radars.

The bow-tie has a flare angle of 80° and the length of each bowtie arm is 13.5 cm. The end resistors are 200 Ω each. The antennas are enclosed in rectangular conducting cavities to reduce direct coupling. The antenna is at the open side of the cavity and the resistors are connected to the cavity wall. The dimensions of the cavity are $l = 33.75$ cm, $w = 28.5$ cm, and $h = 7.5$ cm. The two antennas are

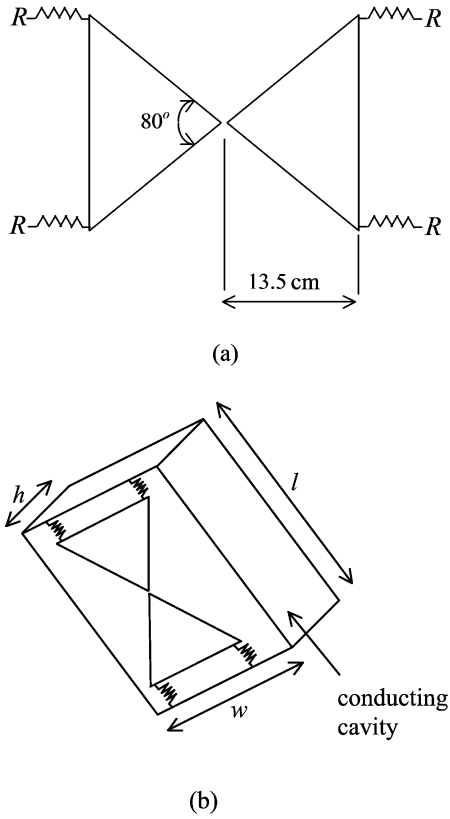

Figure 1. (a) Bow-tie antenna. (b) Antenna with cavity.

placed side-by-side 1.5 cm above the ground with 3 cm gap between the two as shown in Fig. 2.

Aiming at a good signal detection with a low clutter, suitable antenna parameters are chosen from the study in [15]. The input voltage to the transmitting antenna is a Gaussian pulse:

$$V_{inc} = 100 \exp\left(-\frac{t^2}{2\tau_p^2}\right) \tag{1}$$

where V_{inc} is in Volts and the characteristic time of the pulse is $\tau_p = 0.247$ ns (see Fig. 3).

Simulations are done for two soil types: Puerto Rico and San Antonio clay loams, whose dispersive properties have been characterized experimentally in [4]. These soil properties are modeled by a two term Debye model with a static conductivity and the model

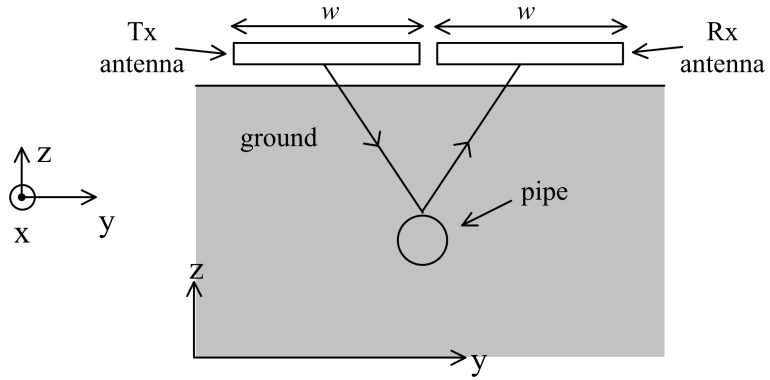

Figure 2. Antennas placed above the ground.

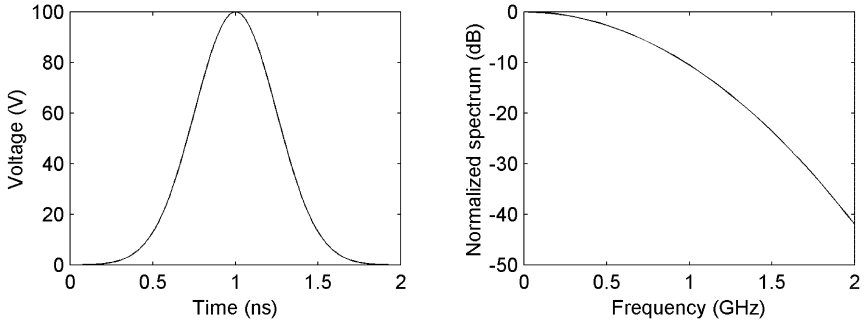

Figure 3. Input signal to the transmitting antenna and its frequency spectrum.

parameters are found by curve fitting the experimental data over the frequency range DC-2 GHz, which is the frequency band of operation of the radar. The complex relative permittivity ε_r of the two term Debye model is given below:

$$\varepsilon_r(\omega) = \varepsilon_\infty + \sum_{i=1}^{2} \frac{G_i(\varepsilon_s - \varepsilon_\infty)}{1 + j\omega t_i} + \frac{\sigma_s}{j\omega\varepsilon_0} \tag{2}$$

where ω is the angular frequency, ε_s is the relative permittivity at DC, ε_0 is the permittivity of free space, ε_∞ is the relative permittivity at $\omega = \infty$, $t_i (i = 1, 2)$ are the Debye relaxation times, σ_s is the static electric conductivity, and $\sum_{i=1}^{2} G_i = 1$. The comparison of the measured

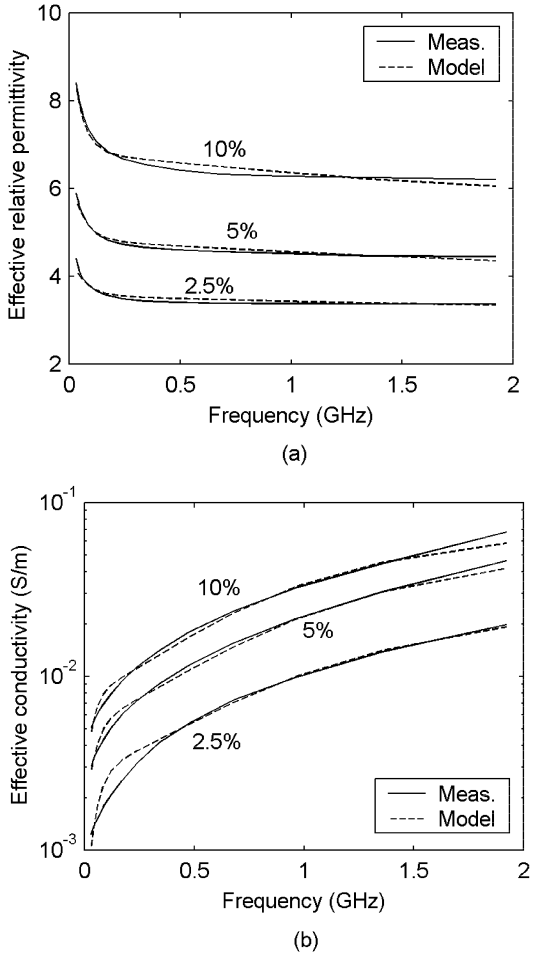

Figure 4. Comparison of measured soil properties with the model for 1.4% dry density Puerto Rico clay loams. Percentages in the figure indicate the moisture contents.

soil properties with the model is shown in Fig. 4 and 5. Tables 1 and 2 give the model parameters where $A_i = G_i(\varepsilon_s - \varepsilon_\infty)$, $(i = 1, 2)$. It can be seen in Figs. 4 and 5 that the model fits the data reasonably well.

The computational domain is divided into cubic cells of size $\Delta = 0.75\,\text{cm}$. The time step Δt is taken as $\Delta t = \Delta/2c = 12.5\,\text{ps}$, where c is the speed of light in free space. Δ and Δt satisfy the Courant condition for numerical stability [16]. Conformal modeling described in

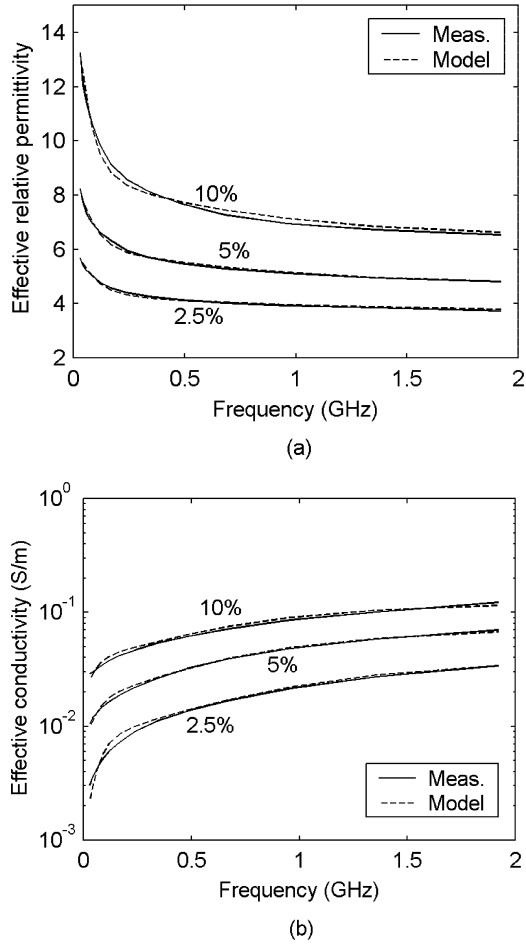

Figure 5. Comparison of measured soil properties with the model for 1.4% dry density San Antonio clay loams. Percentages in the figure indicate the moisture contents.

[17] is used to model the slanted edges of the bow-tie arms. This subcell model is used, as the staircasing is not sufficient to accurately model the edges where the electric and magnetic fields are quite complicated. The input pulse is given to the transmitting antenna through a 200 Ω parallel wire transmission line. This is modeled in FDTD by the 'one way injector model' [14]. This is also used at the receiving antenna by making the input current and voltage zero. The same time and spatial

Table 1. Model parameters for Puerto Rico clay loams.

Moisture	ε_∞	A_1	A_2	t_1 (ns)	t_2 (ns)	σ_s (mS/m)
2.5%	3.201	0.750	0.298	2.297	0.087	0.558
5%	4.048	1.200	0.667	2.386	0.090	2.063
10%	5.706	2.219	0.958	3.100	0.110	3.022

Table 2. Model parameters for San Antonio clay loams.

Moisture	ε_∞	A_1	A_2	t_1 (ns)	t_2 (ns)	σ_s (mS/m)
2.5%	3.635	1.667	0.482	1.700	0.120	1.400
5%	4.589	2.725	1.045	1.850	0.158	8.500
10%	6.310	6.150	1.685	2.300	0.174	22.000

steps as in the main grid are used here.

The dispersion and conductivity in the ground are included in the FDTD algorithm by using the auxiliary differential equation method [9, 10]. UPML [11–13] is used to terminate the computational domain. In this paper, the dispersion is modeled by a two term Debye model with an additional static conductivity. The order of the differential equations is kept at two by suitably selecting the constitutive relationships to decouple the frequency-dependent terms in the Maxwell's equations. The PML used is eight cells thick and a 4th order loss grading is applied over it. The optimum value for the maximum conductivity (normalized with respect to the relative permittivity) in the layer is found from the following equation [12]:

$$\sigma_{\max} \approx \frac{(m+1)}{150\pi\Delta\sqrt{\varepsilon_r}} \tag{3}$$

where m is the order of the loss grading, Δ is the spatial cell size, and ε_r is the relative permittivity of the medium to be matched. For soil, static relative permittivity (ε_s) is taken as the value for ε_r. When PMLs face both the ground and the air, an average value of ε_r is chosen to find $\sigma_{\max}$.

In order to verify the FDTD code for UPML and ADE method, the antenna input impedance is compared with [15] where Berenger PML is used. The antenna parameters are:

flare angle = 70°, length of a bow-tie arm = 13.5 cm, height of antennas above the ground=0.75 cm, cavity dimensions, $l = 33.75$ cm, $w = 24$ cm, $h = 7.5$ cm, separation between the antennas = 3 cm, lump resistors = 200 Ω.

Since the ground medium considered is lossless and nondispersive with $\varepsilon_r = 4$, parameters in the debye model take the following values: relaxation times, $t_1 = t_2 = 0$, $\varepsilon_s = \varepsilon_\infty = 4$, $\sigma_s = 0$, $A_1 = 0$, and $A_2 = 0$.

Fig. 6 shows the comparison. The difference between the two plots is not even discernible. Thus the validity is verified.

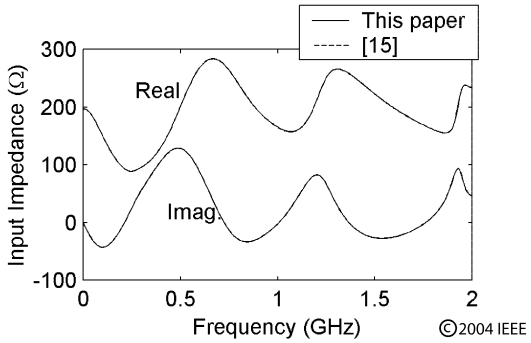

Figure 6. Comparison of input impedance of the transmitting antenna calculated by using different FDTD algorithms.

3. SIMULATION RESULTS

3.1. Smooth Ground Surface with No Inhomogeneities in Soil

First, the GPR is simulated assuming no ground surface roughness and no soil inhomogeneities. The target detected is a pipe buried symmetrically below the two antennas (along x-direction) at a depth of 84 cm. (Pipe depth is kept constant in all the simulations in the paper.) The pipe is modeled in FDTD using the staircase method. The GPR response is calculated for both metal and air-filled plastic pipes where the metal pipe is assumed to be perfectly conducting and the relative permittivity of plastic is taken as $\varepsilon_r = 2$.

Fig. 7 shows the received signals when an eight-inch diameter pipe is buried in Puerto Rico clay loams. Results are shown for 2.5%, 5%, and 10% moisture contents in soil. It can be seen from the figure that the received signal strength decreases with the moisture content in the soil. This happens as the moisture content increases the losses in the

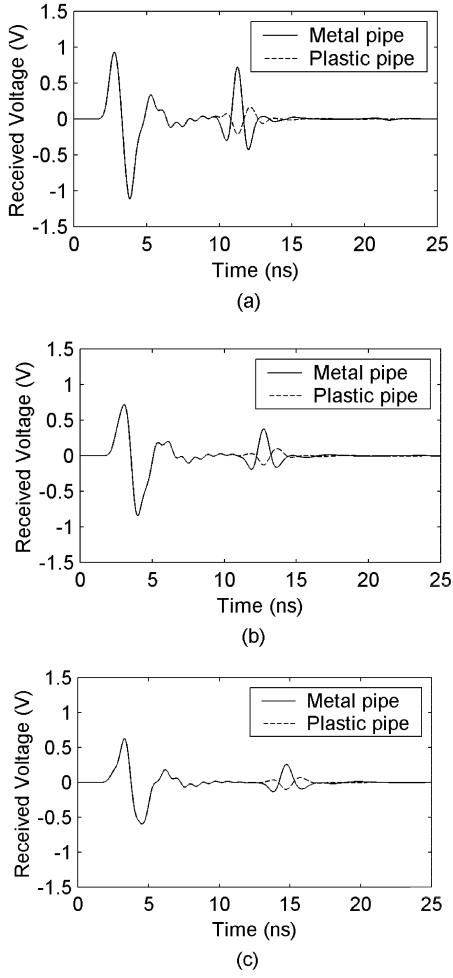

Figure 7. Comparison of the received signals for Puerto Rico clay loams with different moisture contents. (a) 2.5%. (b) 5%. (c) 10%.

soil. Another effect of moisture content is to increase the effective relative permittivity which delays the received scattered signal. Since plastic is a poor reflector of electromagnetic waves, its scattered signal is weak compared to metal as the figure shows.

Fig. 8 shows the same type of simulations for San Antonio clay loams. This soil type has relatively high permittivity values and conductivities compared to Puerto Rico (see Figs. 4 and 5). Therefore the scattered signals are fairly weak and visual detection is almost

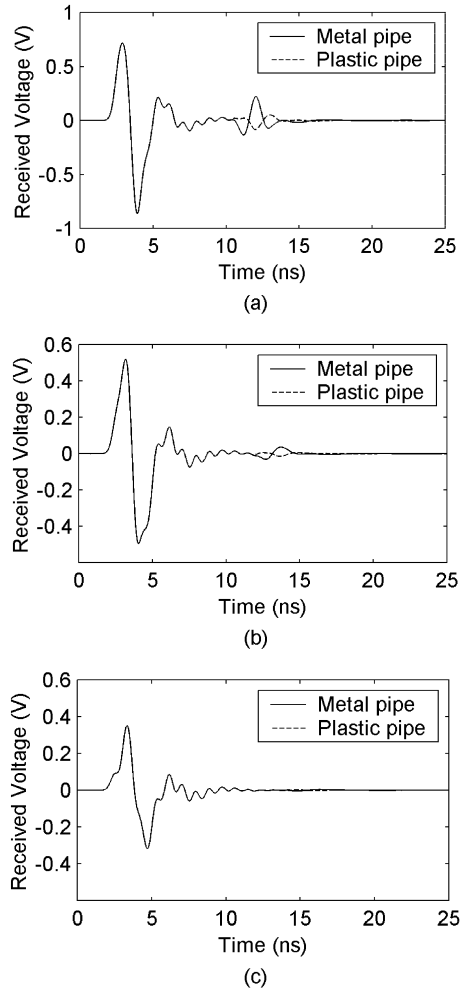

Figure 8. Comparison of the received signals for San Antonio clay loams with different moisture contents. (a) 2.5%. (b) 5%. (c) 10%.

impossible for the case of 10% moisture content. Fig. 9 shows the scattered signal found in this case by subtracting the clutter from the total received signal. The received scattered signal is in the order of a few millivolts. To find the clutter in a practical situation, the radar can be moved away from the target and readings can be obtained at several positions on the ground. The average reading would give a reasonable value for the clutter provided the ground is

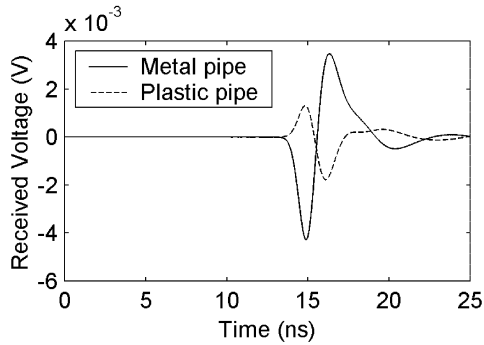

Figure 9. Scattered signals from pipes in San Antonio clay loam with 10% moisture content.

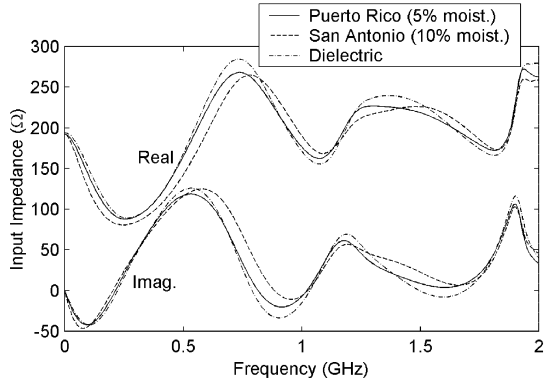

Figure 10. Comparison of the input impedances of the transmitting antenna for different ground conditions.

fairly homogeneous. Otherwise, an advanced detection algorithm has to be used to pick the target echo.

It is clear from Figs. 7, 8, and 9 that metal and plastic pipes give two unique scattered signal shapes irrespective of the ground conditions. The shapes agree well with the results published in [8]. These target signatures can be used to distinguish between metal and plastic pipes. Also this prior knowledge of target echo is essential for the application of frequency domain signal processing techniques for better target detection.

Fig. 10 compares the input impedances of the transmitting antenna of the GPR for three different ground conditions, i.e.,

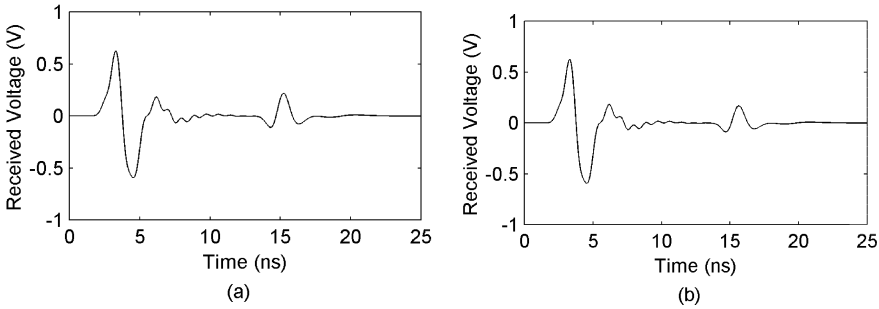

Figure 11. The received signals when metal pipes of different size are buried in Puerto Rico clay loams with 10% moisture. (a) 6-inch diameter. (b) 4-inch diameter.

5% moisture Puerto Rico, 10% moisture San Antonio, and lossless nondispersive material with $\varepsilon_r = 4$. The antenna input impedance is not considerably affected by the properties of the ground above which the antenna is operating. It depends mainly on the flare angle and the lump resistors [15]. This is an important feature in a GPR antenna which operates in many different ground conditions.

Next, simulations are done for different pipe sizes. Received signals of two such cases are shown in Fig. 11. The pipe diameters are 6 and 4 inches and are buried in Puerto Rico clay loams having a moisture content of 10%.

Fig. 12 shows how the GPR response changes when the two antennas are moved along a line normal to the pipeline. The pipe is metal and has a diameter of 8 inches. The antennas are moved 90 cm in steps of 7.5 cm over the pipe. The soil type is Puerto Rico with 10% moisture.

Next, target polarization properties are investigated. If an incident electric field has components E_x^i and E_y^i along x and y directions respectively, then the corresponding scattered electric field components E_x^s and E_y^s are given by

$$\begin{pmatrix} E_x^s \\ E_y^s \end{pmatrix} = \begin{pmatrix} S_{xx} & S_{xy} \\ S_{yx} & S_{yy} \end{pmatrix} \begin{pmatrix} E_x^i \\ E_y^i \end{pmatrix} \tag{4}$$

where S_{xx}, S_{xy}, S_{yx}, and S_{yy} are scattering parameters. For a long thin target like a pipe, when aligned along the x direction, S_{xy} and S_{yx} are very small. For a metal pipe $S_{xx} > S_{yy}$ and for a plastic pipe, since its permittivity is less than that of surrounding soil, $S_{yy} > S_{xx}$ [18]. Simulations done with the 8-inch diameter pipe aligned along the

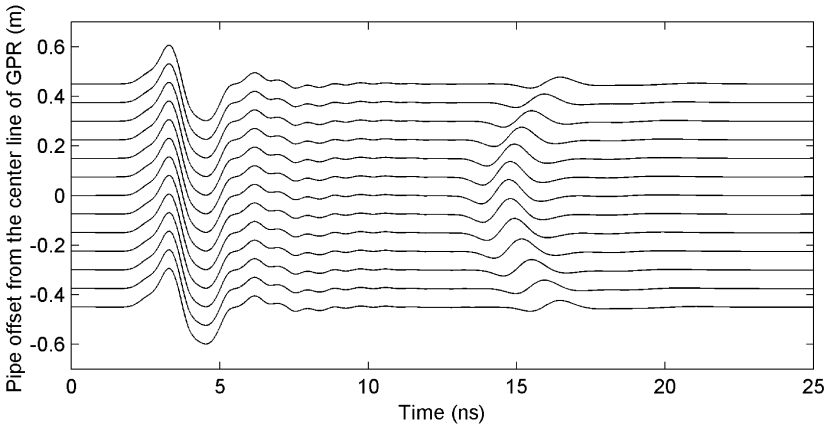

Figure 12. Variation of the GPR response when the two antennas are moved along a line perpendicular to the pipe.

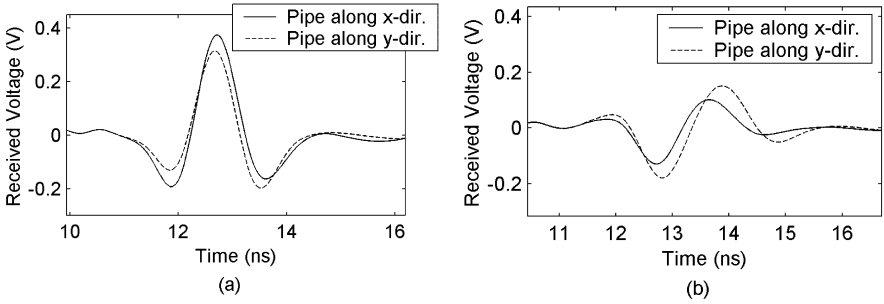

Figure 13. Comparison of the scattered signals when the pipe aligned along the x and y directions. (a) Metal pipe. (b) Plastic pipe.

x and y directions, agree very well with this theory. Fig. 13 shows the enlarged scattered signals in the 5% moisture Puerto Rico clay loams. According to the figure, for the metal pipe, the scattered signal is larger when the pipe is aligned along the x direction than it is when the pipe is aligned along the y direction. For the plastic pipe it is vise versa.

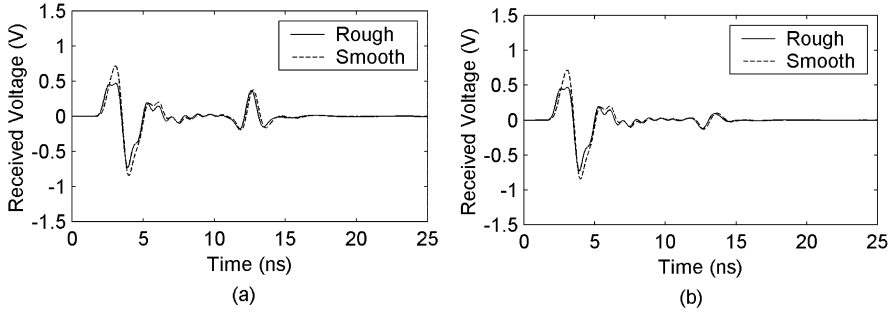

Figure 14. Comparison of the received signals with and without surface roughness for Puerto Rico clay loams with 5% moisture content. (a) Metal pipe. (b) Plastic pipe.

3.2. Effect of Surface Roughness and Soil Inhomogeneities

3.2.1. Surface Roughness

First, the surface roughness is added to the air ground interface to find what effect it has on the GPR response. This is simulated by adding rectangular holes of different sizes to the ground surface. In the computational domain, the ground surface has a size of $75\Delta \times 100\Delta$ (56.25 cm $\times$ 75.5 cm) and 100 holes are randomly placed on it. The length and width of holes vary from $2\Delta - 9\Delta$ (1.5 cm–6.75 cm) and the depth varies from $2\Delta - 5\Delta$ (1.5 cm–3.75 cm). Figs. 14 and 15 shows the simulation results for Puerto Rico and San Antonio type soils with a 5% moisture content respectively. The target detected is an 8-inch diameter metal pipe.

The results show that the addition of surface roughness has distorted the pulse in early time signals which mainly consists of the ground surface reflection. But the scattered signal from the pipe is mostly unaffected. Also it has not increased the signal ringing period. Therefore, the detectability of the pipes by the GPR is not harmed by the surface roughness. Similar results could be observed for soils with other moisture contents.

3.2.2. Surface Roughness and Inhomogeneities

Next, soil inhomogeneities with different sizes and material properties are added to the soil randomly. 120 such scatterers are placed as shown in Fig. 16. Their lengths, widths, and heights are varied in the range $\Delta - 5\Delta$ (0.75 cm–3.75 cm). These inhomogeneities are assumed to be lossy and nondispersive and their relative permittivity values

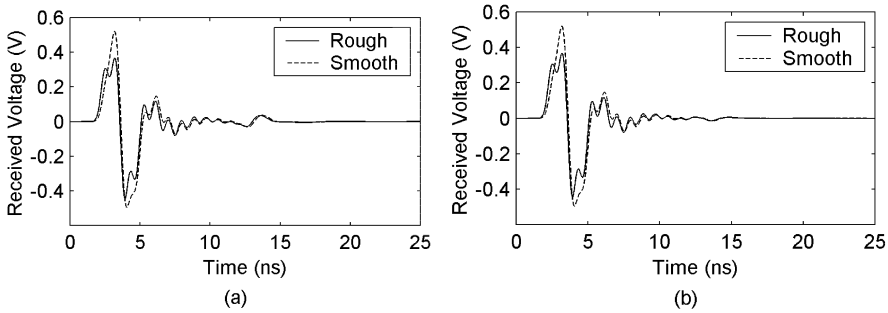

Figure 15. Comparison of the received signals with and without surface roughness for San Antonio clay loams with 5% moisture content. (a) Metal pipe. (b) Plastic pipe

are taken in the range 5–15. Generally, the inhomogeneities closer to the ground surface have higher conductivities due to the presence of organic material. Therefore, conductivities in the range 0.1–0.4 S/m are selected for the scatterers not deeper than 15 cm. The other scatterers are given conductivities in the range 0.04–0.08 S/m.

Simulations are done when both surface roughness and inhomogeinieties are present in order to find the detectability of the target. The results show that the scatterers have negligible effect on the GPR response when compared to the surface roughness. Fig. 17 shows the received signals when an 8-inch diameter pipe is buried in Puerto Rico and San Antonio clay loams with 5% moisture content. Small scatterers spread all over the soil cannot mask the target echo coming from the pipe. If the target is as small as the scatterers, visual detection would be almost impossible and more advanced detecting algorithms in frequency domain would have to be used to pick the target echo.

4. CONCLUSION

A complete 3-D FDTD simulation of a realistic GPR operating above lossy and dispersive media is described. The antenna is a resistor-loaded bow-tie which is a widely used broadband antenna in commercial GPRs. The simulation results show the detection of metal and plastic pipes, buried in Puerto Rico and San Antonio clay loams. Ground surface roughness and soil inhomogeneities are also included to simulate a real application.

The effect of moisture content, ground surface roughness, and soil inhomogeneities on the GPR response is described in the paper. It is

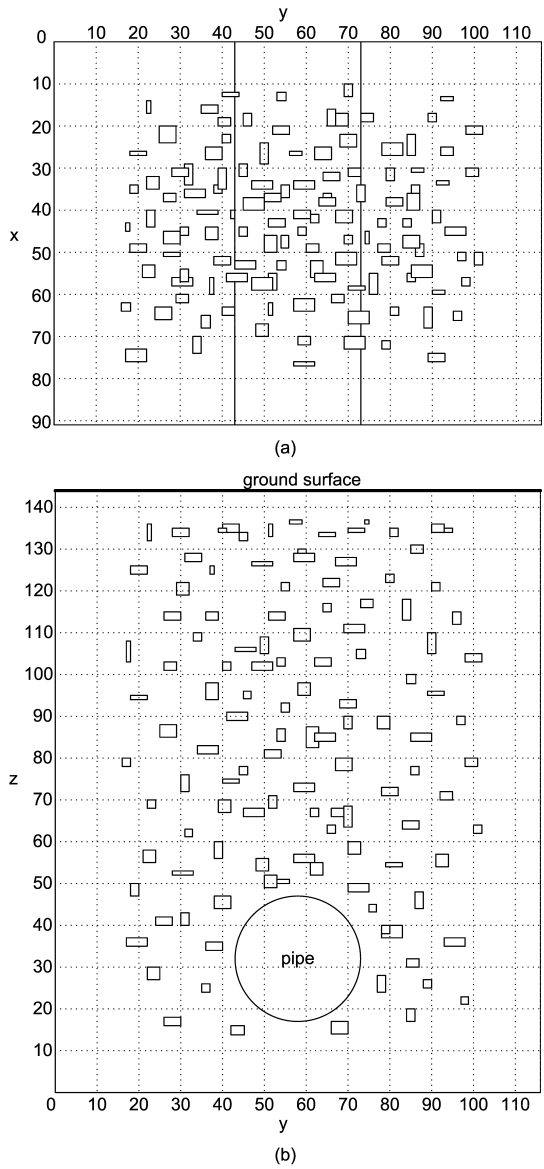

Figure 16. Positions of soil inhomogeneities in the computational domain. (a) View above the ground. (b) Sectional view through the ground. (The scale is in number of cells.)

clear from the results that the surface roughness has a larger impact on the GPR response than the inhomogeneities, but neither of them masks the echo of the buried pipes. The simulations also present important information like target signatures, target polarization properties, and effect of soil properties on the antenna input impedance.

Modeling of a realistic GPR of this nature is useful for the development of more advanced radar hardware and signal processing techniques. Especially the calculated scattered signals can be used to find their spectrums and resonances so that frequency domain detection algorithms can be applied.

ACKNOWLEDGMENT

Swedish International Development Cooperation Agency (SIDA) is gratefully acknowledged for providing the financial support of this work. Thanks also to the center for parallel computing (PDC) at the Royal Institute of Technology for providing necessary computer resources.

REFERENCES

1. Yee, K. S., "Numerical solution of initial boundary value problems involving Maxwells equations in isotropic media," *IEEE Trans. Antennas Propagat.,* Vol. AP-14, 302–307, May 1966.
2. Taflove, A., *Computational Electrodynamics,* Artech House, 1995.

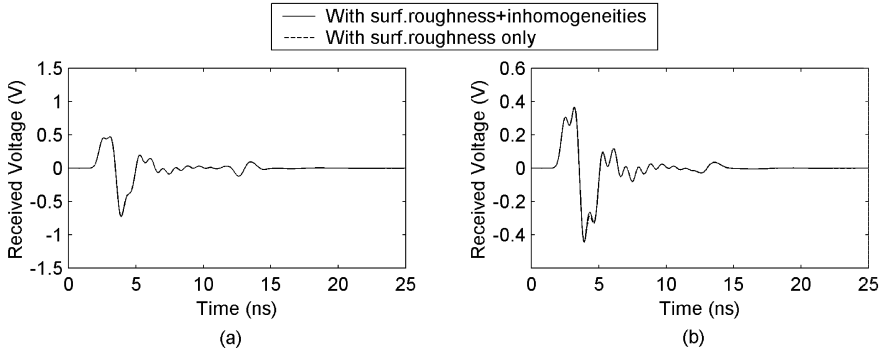

Figure 17. Effect of the soil inhomogeneities on the GPR response (a) 5% moisture Puerto Rico with the plastic pipe. (b) 5% moisture San Antonio with the metal pipe.

3. Taflove, A., *Advances in Computational Electrodynamics,* Artech House, 1998.
4. Hipp, J. E., "Soil electromagnetic parameters as functions of frequency, density, and soil moisture," *Proc. IEEE,* Vol. 62, 98–103, Jan. 1974.
5. Gurel, L. and U. Oguz, "Simulations of ground penetrating radars over lossy and heterogeneous grounds," *IEEE Trans. Geosci. Remote Sensing,* Vol. 39, 1190–1197, June 2001.
6. Oguz, U. and L. Gurel, "Frequency responses of ground penetrating radars operating over highly lossy grounds," *IEEE Trans. Geosci. Remote Sensing,* Vol. 40, 1385–1394, June 2002.
7. Teixeira, F. L., W. C. Chew, M. Straka, M. L. Oristaglio, and T. Wang, "Finite-difference time domain simulation of ground penetrating radar on dispersive, Inhomogeneous, and conductive soils," *IEEE trans. Geosci. Remote Sensing,* Vol. 36, 1928–1937, Nov. 1998.
8. Bourgeois, J. M. and G. S. Smith, "A fully three-dimensional simulation of a ground-penetrating radar: FDTD theory compared with experiment," *IEEE Trans. Geosci. Remote Sensing,* Vol. 34, 36–44, Jan. 1996.
9. Kashiwa, T. and I. Fukai, "A treatment by FDTD method of dispersive characteristics associated with electronic polarization," *Microwave and Optics Technology Letters,* Vol. 3, 203–205, 1990.
10. Joseph, R. M., S. C. Hagness, and A. Taflove, "Direct time integration of Maxwell's equations in linear dispersive media with absorption for scattering and propagation of femtosecond electromagnetic pulse," *Optics Letters,* Vol. 16, 1412–1414, 1991.
11. Sacks, Z. S., D. M. Kingsland, R. Lee, and J. F. Lee, "A perfectly matched anisotropic absorber for use as an absorbing boundary condition," *IEEE Trans. Antennas Propagat.,* Vol. 43, 1460–1463, Dec. 1995.
12. Gedney, S. D., "An anisotropic perfectly matched layer-absorbing medium for the truncation of FDTD lattices," *IEEE Trans. Antennas Propagat.,* Vol. 44, 1630–1639, Dec. 1996.
13. Gedney, S. D., "An anisotropic PML absorbing media for FDTD simulation of field in lossy dispersive media," *Electromagnetics,* Vol. 16, 399–415, 1996.
14. Maloney, J. G., K. L. Shlager, and G. S. smith, "A simple FDTD model for transient excitation of antennas by transmission lines," *IEEE Trans. Antennas Propagat.,* Vol. 42, 289–292, Feb. 1994.
15. Uduwawala, D., M. Norgren, P. Fuks, and A. Gunawardena, "A

deep parametric study of resistor-loaded bow-tie antennas for ground penetrating radar applications using FDTD," *IEEE Trans. Geosci. Remote Sensing,* Vol. 42, No. 4, 732–742, April 2004.

16. Taflove, A. and M. E. Brodwin, "Numerical solution of steady-state electromagnetic scattering problems using the time-dependent Maxwells equations," *IEEE Trans. Microwave Theory Tech.,* Vol. MTT-23, 623–630, Aug. 1975.
17. Jurgens, T. G., A. Taflove, K. Umashankar, and T. G. Moore, "Finite-difference time-domain modeling of curved surfaces," *IEEE Trans. Antennas Propagat.,* Vol. 40, 357–366, April 1992.
18. Daniels, D. J., D. J. Gunton, and H. F. Scott, "Introduction to subsurface radar," *IEEE Proc.,* Vol. 135, Pt. F, No. 4, 278–320, Aug. 1988.

Disala Uduwawala was born in Kandy, Sri Lanka, on December 25, 1973. He received the B.S. degree in Electrical and Electronic Engineering from the University of Peradeniya, Sri Lanka in 1999 and the Technical Licentiate degree from the Royal Institute of Technology, Stockholm, Sweden in 2004. At present, he is pursuing the Ph.D. degree from the Royal Institute of Technology. His research interests are computational methods in electromagnetism and antenna design for subsurface radars.

Martin Norgren received the Dr. Tech degree in electromagnetic theory from the Royal Institute of Technology, Stockholm, Sweden, in 1997. He is currently an Associate Professor with the Division of Electromagnetic Theory, Royal Institute of Technology. His current research interests are electromagnetic theory in general, with special interests in waveguiding problems and scattering problems involving complicated materials, and the related inverse scattering problems and inverse source problems.

Peter Fuks was born in Swidnica, Poland, on March 8, 1949. He received the M.S.E.E. and Ph.D. degrees from the Royal Institute of Technology, Stockholm in 1973 and 1982, respectively. Since 1973, he has been with the Royal institute of Technology in various research and teaching positions. His main scientific interests are in broadband antennas

Aruna Gunawardena received the B.S. degree (with honors) in Electrical and Electronic Engineering from the University of Peradeniya, Sri Lanka in 1986, the MEng.Sc. degree in

Communications Engineering from the University of New South Wales, Australia in 1991, and the Ph.D. degree in Electrical Systems Engineering from the University of Queensland, Australia in 1997. Between 1996 and 1999, he worked as a Research Fellow at the Cooperative Research Center for Sensor Signal and Information Processing (CSSIP) Australia and his work was mainly focused on the image processing of synthetic aperture (SAR) data. Since 1999, he has been with the Department of Electrical and Electronic Engineering at the University of Peradeniya where he is currently a Senior Lecturer. His main research interests are in the areas of digital signal and image processing and radar system design.